Abundance Recovery Error Analysis using Simulated AVIRIS Data

William W. Stoner, Joseph C. Harsanyi, William H. Farrand and Jennifer A. Wong

Science Applications International Corporation
803 West Broad Street
Falls Church VA,22046

1.0 Introduction

Measurement noise and imperfect atmospheric correction translate directly into errors in the determination of the surficial abundance of materials from imaging spectrometer data. The effects of errors on abundance recovery have been investigated previously using Monte Carlo simulation methods by Sabol et. al. [1]. The drawback of the Monte Carlo approach is that thousands of trials are needed to develop good statistics on the probable error in abundance recovery. This computational burden invariably limits the number of scenarios of interest that can practically be investigated.

A more efficient approach is based on covariance analysis. The covariance analysis approach expresses errors in abundance as a function of noise in the spectral measurements and provides a closed form result eliminating the need for multiple trials. In this paper, Monte Carlo simulation and covariance analysis are used to predict confidence limits for abundance recovery for a scenario which is modeled as being derived from AVIRIS.

2.0 Abundance Recovery Error Derivation

The visible and near infrared reflectance vector of a surface, $\underline{\mathbf{R}}$, is the product of an n x m matrix **M** of endmember spectra and an m x 1 abundance vector $\underline{\mathbf{A}}$

$$\underline{\mathbf{R}} = \mathbf{M}\underline{\mathbf{A}}$$

For simplicity, we assume Lambertian properties for the modeled pixel surface, and we also assume that the surface is level. With these assumptions, we use the n x n diagonal matrices **L** and **T** to represent the surface irradiance and atmospheric transmission between the surface and the sensor respectively. The ground reflected radiance at the sensor is represented by the n x 1 vector $\mathbf{LT}\underline{\mathbf{R}} = \mathbf{LTM}\underline{\mathbf{A}}$.

In addition to the multiplicative effects on the reflectance vector, upwelling light from thermal radiation and atmospheric scattering is represented by an additive term given by the n x 1 vector $\underline{\mathbf{U}}$. The total upward radiance (represented by the n x 1 vector $\underline{\mathbf{D}}$) is now given as

$$\underline{\mathbf{D}} = \mathbf{TLM}\underline{\mathbf{A}} + \underline{\mathbf{U}} + \underline{\mathbf{N}}$$

where $\underline{\mathbf{N}}$ is an n x 1 zero mean additive white Gaussian noise vector with covariance $\Sigma_N = \sigma^2\mathbf{I}$ where **I** is the n x n identity matrix and σ^2 is the noise variance.

The first step in the recovery process is estimation of the atmospheric contributions, denoted by $\hat{\mathbf{T}}\hat{\mathbf{L}}$ and $\hat{\underline{\mathbf{U}}}$. Errors in estimation of these quantities will tend to bias abundance recovery results as well as increase the size of the resultant error distribution.

From a theoretical standpoint, it is useful to consider the case where the atmospheric contributions are perfectly estimated, and the only error is due to random effects such as sensor noise. The equation with the atmospheric effects removed becomes

$$(\mathbf{TL})^{-1}(\underline{\mathbf{D}}-\underline{\mathbf{U}}) = \mathbf{M}\underline{\mathbf{A}}+(\mathbf{TL})^{-1}\underline{\mathbf{N}}$$

The least squares estimate $\hat{\underline{\mathbf{A}}}$ is given by the well known result [2]

$$\hat{\underline{\mathbf{A}}} = (\mathbf{M}^{\mathrm{T}}\mathbf{M})^{-1}\mathbf{M}^{\mathrm{T}}\left((\mathbf{TL})^{-1}(\underline{\mathbf{D}}-\underline{\mathbf{U}})\right) = \underline{\mathbf{A}}+(\mathbf{M}^{\mathrm{T}}\mathbf{M})^{-1}\mathbf{M}^{\mathrm{T}}(\mathbf{TL})^{-1}\underline{\mathbf{N}}$$

The variance-covariance matrix of $\hat{\underline{\mathbf{A}}}$ is given by

$$\mathrm{Var}(\hat{\underline{\mathbf{A}}}) = (\mathbf{M}^{\mathrm{T}}\mathbf{M})^{-1}\mathbf{M}^{\mathrm{T}}(\mathbf{TL})^{-1}\Sigma_{\mathbf{N}}((\mathbf{M}^{\mathrm{T}}\mathbf{M})^{-1}\mathbf{M}^{\mathrm{T}}(\mathbf{TL})^{-1})^{\mathrm{T}}$$

The square roots of the eigenvalues of this matrix are the semi-axes of a hyperdimensional ellipsoid which describes the error distribution of the recovered abundances. The eigenvectors determine the orientation of the ellipsoid. This representation of the abundance estimation error provides a closed form solution for assessing the confidence that the true abundance vector lies within particular limits.

3.0 Simulation Results

Laboratory spectra of a red soil, creosote leaves and dry grass were used to simulate a mixed pixel. The resulting mixed pixel reflectance spectrum was convolved with gains and offsets previously calculated by a simulated empirical line method calibration [3] of the same pixel. The earlier simulation convolved the mixed pixel with the multiplicative and additive effects of a mid-latitude summer atmosphere illuminated with a solar zenith angle of 30^{o} as calculated by the LOWTRAN 7 radiative transfer code. The instrumental response of AVIRIS was simulated for the input radiance vector with the output vector consisting of 224 digital numbers corresponding to AVIRIS channels. Additive noise with standard deviation of 5 DN (representing AVIRIS performance circa 1987-1988) was added to the simulated raw AVIRIS data, and the same gains and offsets were used to convert the data back to reflectance providing a perfect atmospheric correction. Finally, the abundances were solved for using singular value decomposition based least squares techniques [4].

Figure 1a shows the projection of the simulation derived error distribution onto 2D planes relating errors in pairs of abundance measurements. Figure 1b shows the theoretical 95% confidence ellipsoid projected onto 2D planes for the same scenario. In order to obtain results comparable to the theoretical error distributions, approximately 10000 trials were needed to obtain the required statistics. The run-time for 10000 trials is approximately two orders of magnitude greater than the theoretical calculation (e.g. 1000 sec vs. 10 sec on a 486 PC).

4.0 Conclusion

The example shown here demonstrates that the orientation and size of an abundance recovery error ellipsoid can be determined accurately with covariance analysis. This approach eliminates the need to generate statistics from which to calculate the error covariance matrix reducing the calculation to a small fraction of the computational burden of the Monte Carlo simulation approach. In further investigations that simulated the current, higher SNR configuration of AVIRIS, the abundance recovery error is

significantly reduced. Thus, given a higher SNR sensor system, greater confidence can be invested in spectral mixture studies.

Acknowledgments
Laboratory spectra used in this study were measured at Brown University's RELAB and at the University of Washington's Remote Sensing Laboratory.

References

[1] Sabol D.E., J.B. Adams and M.O. Smith (1990) Predicting the Spectral Detectability of Surface Materials using Spectral Mixture Analysis: *Proc. of IGARSS '90 Symposium*, 2, 967-970.
[2] Menke, W. (1989) *Geophysical Data Analysis: Discrete Inverse Theory*, Academic Press Inc., San Diego.
[3] Conel, J.E. and R.E. Alley (1985) Lisbon Valley, Utah uranium test site report. *The Joint NASA/Geosat Test Case Project.* H.N. Paley (ed.)
[4] Press, W.H., B.P. Flannery, S.A. Teukolsky and W.T. Vetterling (1986) *Numerical Recipes*, Cambridge University Press, New York.

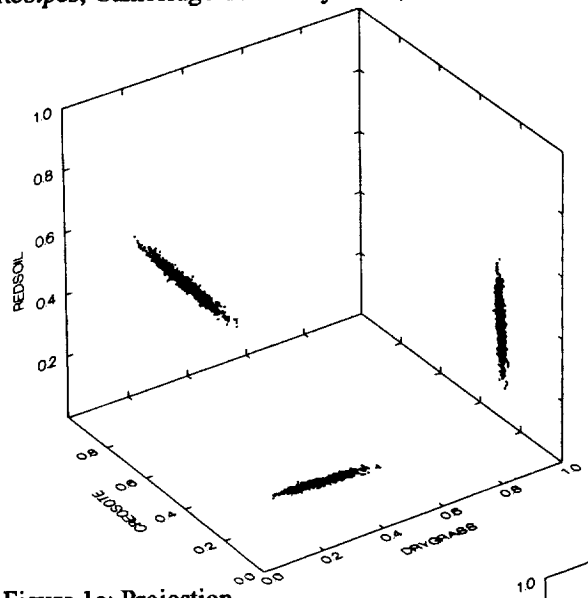

Figure 1a: Projection of 3D Scatter Plot of Abundance Estimates onto 2D planes for case with Red Soil (30%), Creosote Leaves (30%) and Dry Grass (40%).

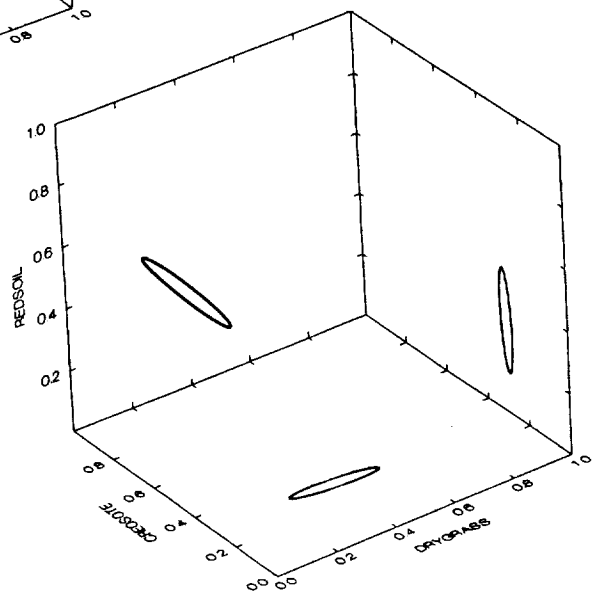

Figure 1b: Theoretical Abundance Recovery Error Ellipsoid for above case projected onto 2D planes. 95% confidence level is represented.